

Heat capacity evidence for conventional superconductivity in the Type-II Dirac semi-metal PdTe₂

Amit and Yogesh Singh

Department of Physical Sciences, Indian Institute of Science Education and Research (IISER) Mohali, Knowledge City, Sector 81, Mohali 140306, India.

(Dated: November 30, 2021)

We use electrical transport, magnetoresistance, and heat capacity measurements on high quality single crystals of the recently discovered superconducting Type-II Dirac semi-metal PdTe₂, to probe the nature of its superconducting phase. The magnitude of the electronic heat capacity anomaly at T_c , the low temperature exponential T dependence of the heat capacity, and a conventional $H - T$ phase diagram establish that the superconductivity in PdTe₂ is conventional in nature despite the presence of a topologically non-trivial Fermi surface band which contributes to the electrical conduction.

Topological superconductors have been the focus of intense recent research¹. This is in part due to the possibility that these materials may host Majorana Fermion excitations^{2,3} which, in addition to being of fundamental interest, can also be used in fault tolerant Quantum computation. To stabilize topological superconductivity various routes have been pursued. For example, doping⁴⁻¹¹ or pressurizing¹² a parent topological material, studying chiral spin-triplet superconductors¹³, making heterostructures of a semi-conductor with a conventional superconductor^{14,15}, or a topological material with a conventional superconductor^{16,17}. Another exciting new avenue has opened up in which superconductivity has been shown to emerge in nano-scale point contacts between. Topological materials and normal metals¹⁸⁻²⁰.

In all these routes, superconductivity is induced by some tuning like doping, pressure, proximity, or confinement. It would be ideal to look for a system in which Topological band structure and superconductivity emerge naturally and to then demonstrate the Topological character of the superconductivity.

Recently, a new family of transition metal dichalcogenide materials AX_2 ($A = \text{Pt, Pd}$, $X = \text{Te, Se}$) have been shown to be Type-II Dirac materials where the electronic band structure consists of a tilted Dirac cone²¹⁻²⁴. This follows the discovery of Type-II Weyl materials²⁵⁻³⁰. Both the Type-II Weyl and Dirac Fermions observed in the above materials break Lorentz invariance and are therefore fundamentally different quasiparticles compared to the normal Type-I Dirac and Weyl Fermions discovered earlier. The study of the properties of these Type-II topological materials are therefore of immense fundamental interest and could lead to important technological applications. How conventional or fairly well understood states of matter like magnetism or superconductivity emerge in materials with Topological band-structures has been an emerging frontier area of research. In this context, PdTe₂ is specially important since it is known to also host a superconducting state below the critical temperature $T_c \approx 1.7 \text{ K}$ ³¹. Topological superconductivity in PdTe₂ is thus an exciting possibility which needs to be carefully examined.

In this work we report electrical transport, magneto-

transport, and heat capacity C measurements on high quality single crystals of the superconducting Type-II Dirac semi-metal PdTe₂ to explore the possible unconventional (Topological) nature of the superconducting state. We confirm superconductivity with a critical temperature $T_c \approx 1.7 \text{ K}$ using electrical transport measurements. From recent Shubnikov de Haas (SdH) oscillations in magneto-transport measurements we have shown that 4 bands contribute to the transport, including a band with a non-trivial Berry phase³². This raises the enticing possibility of Topological superconductivity in PdTe₂. Our heat capacity measurements demonstrate bulk superconductivity below $T_c \approx 1.7 \text{ K}$. The size of the superconducting anomaly in the heat capacity ΔC at T_c is estimated to be $\Delta C/\gamma T_c \approx 1.52$, which is close to the value 1.43 expected for a conventional weak-coupling single-gap BCS superconductor. The $C(T)$ at low temperature shows an exponential T dependence suggesting a fully gapped superconducting state. Additionally, the $C(T)$ data in various applied magnetic fields H is used to construct an $H-T$ phase diagram which also shows a conventional behaviour. Thus, our measurements strongly indicate that the superconductivity in PdTe₂ is conventional in nature despite the presence of Topologically non-trivial electrons contributing to the transport.

Experimental: Single crystals of PdTe₂ were synthesized using a modified Bridgeman method. The starting elements, Pd powder (99.99 % purity) and Te shots (99.9999 %), were weighed in the atomic ratio 1 : 2.2 and sealed in an evacuated quartz tube. The 10% extra Te was taken to compensate for Te loss due to its high vapor pressure. For crystal growth, the tube with the starting materials was heated to 790 °C in 15 h, kept there for 48 h, and then it was slowly cooled to 500 °C over 7 days. They were then annealed at 500 °C for 5 days before cooling naturally. The shiny crystals of millimeter size thus obtained could be cleaved easily from the as grown boule. A typical crystal is shown on a millimeter grid in the inset of Fig. 1. The Chemical composition of crystals was verified by energy dispersive spectroscopy (EDS) on a JEOL SEM. The ratio given by EDS between Pd and Te was 1 : 1.99, showing the stoichiometric ratio of the compound. Few crystals were crushed into

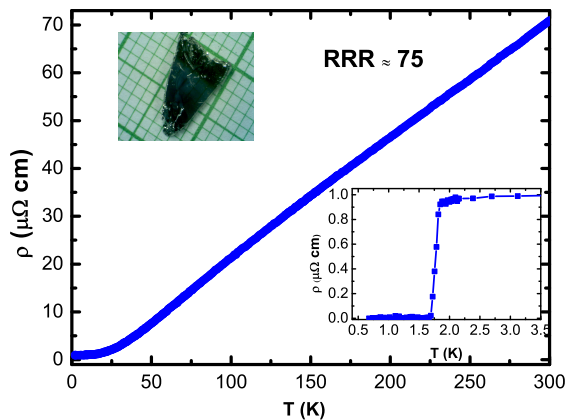


FIG. 1. (Color online) Electrical resistivity ρ versus T for PdTe₂ measured in zero applied magnetic field with a current $I = 0.5$ mA applied in the crystallographic ab -plane. The top inset shows an optical image of a PdTe₂ crystal placed on a millimeter grid. The bottom inset shows the $\rho(T)$ data below 3 K to highlight the superconducting transition with $T_c \approx 1.75$ K.

powder for X-ray diffraction measurements. The powder X-ray diffraction pattern confirm the phase purity of PdTe₂, well crystallized in the CdI₂-type structure with the P3m1(164) space group..

The electrical transport and heat capacity down to 0.4 K were measured using the He3 option of a quantum design physical property measurement system (QD-PPMS).

Electrical Transport: Figure 1 shows the electrical resistivity ρ versus temperature T measured in zero magnetic field with a current $I = 0.5$ mA applied within the crystallographic ab -plane. The $\rho(T)$ shows metallic behaviour with $\rho(300 \text{ K}) \approx 70 \mu\Omega \text{ cm}$ and $\rho(2 \text{ K}) \approx 0.94 \mu\Omega \text{ cm}$, giving a residual resistivity ratio $RRR \approx 75$. This RRR is larger than reported earlier indicating that the PdTe₂ crystals are of high quality. The lower inset in Fig. 1 shows the $\rho(T)$ data below $T = 3$ K and the abrupt drop to zero resistance below $T_c = 1.75$ K confirms the superconductivity in PdTe₂.

We have recently reported³² observation of quantum oscillations in the magneto-transport measurements on PdTe₂ crystals below $T = 20$ K, again suggesting the high quality of the samples. For magnetic field applied perpendicular the c -axis, we observed a single frequency at 419 T in the fast Fourier transform of the dHvA data. The Berry phase for this band was estimated to be non-trivial suggesting its Topological nature. Additionally, 3 other frequencies were observed for $H||c$ -axis. Thus there are multiple electronic bands including a Topological band contributing to the transport and it is unclear from just transport measurements whether the observed superconductivity itself has any unconventional Topological character.

Heat Capacity: We have therefore used heat capacity

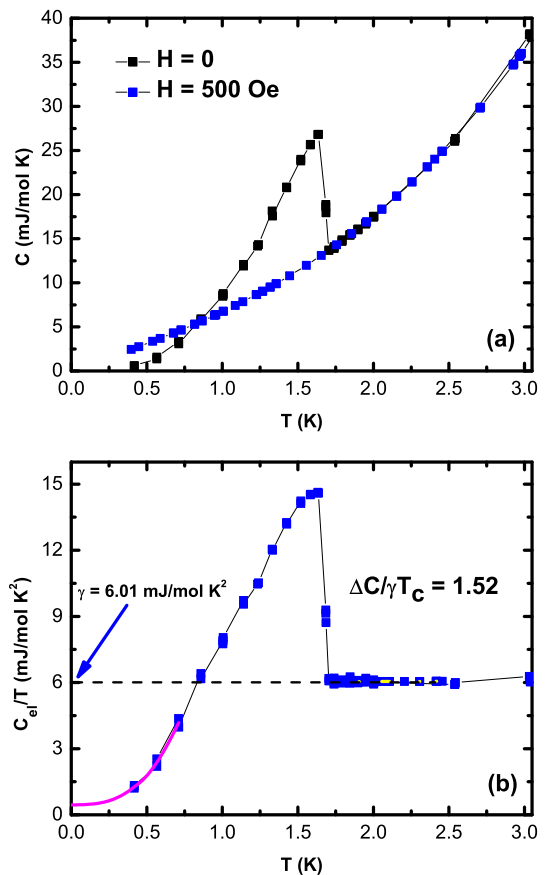


FIG. 2. (Color online) (a) Heat capacity C versus T for PdTe₂ measured in $H = 0$ and $H = 500$ Oe. (b) Electronic contribution to the heat capacity divided by temperature C_{el}/T . The horizontal dash-dot line is the value $\gamma = 6.01$ mJ/mol K² and the solid curve through the lowest T data is a fit by a gapped model (see text for details).

measurements to address the nature of superconductivity in PdTe₂. Figure 2 (a) show the heat capacity C versus temperature T data for PdTe₂ between $T = 0.4$ and 3 K measured in $H = 0$ and $H = 500$ Oe magnetic field. A sharp anomaly at $T_c = 1.72$ K in the $H = 0$ data indicates that the superconductivity previously reported using only transport measurements, is bulk in nature. No anomaly is observed down to the lowest temperatures measured in $H = 500$ Oe, suggesting that the superconductivity has been completely suppressed. This is confirmed by our heat capacity data in various magnetic field which will be presented later. The $H = 500$ Oe data was treated as the normal state data and was fit to the expression $C = \gamma T + \beta T^3$. The fit (not shown) gave the values $\gamma = 6.01(3)$ mJ/mol K² and $\beta = 0.66(1)$ mJ/mol K⁴. The lattice part βT^3 was then subtracted from the $C(T)$ data at $H = 0$ to obtain the electronic part of the heat capacity C_{el} . The electronic heat capacity divided by temperature C_{el}/T versus T is shown in Fig. 2 (b). An extremely sharp transition at the onset of superconductivity is observed

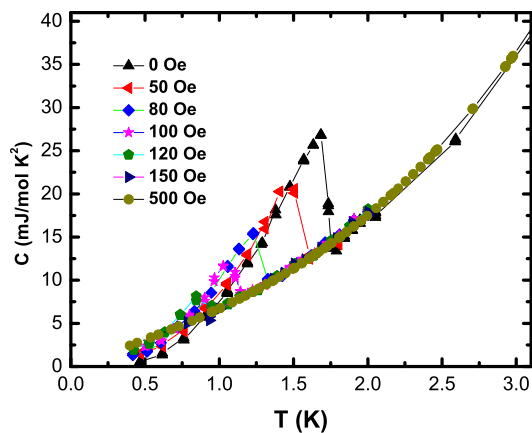


FIG. 3. (Color online) Heat capacity C versus T for PdTe₂ between $T = 0.4$ and 3 K, measured in various magnetic fields H .

at $T_c = 1.72$ K. The normal state Sommerfeld coefficient $\gamma = 6.01$ mJ/mol K² is indicated by an extrapolation (dashed line in Fig. 2 (b)) to $T = 0$ of the normal state data. An equal entropy construction (not shown) gave almost the same $T_c = 1.69$ K, indicating no broadening or smearing out of the superconducting transition due to sample inhomogeneities or imperfections.

The data at the lowest temperatures were fit by the expression $C_{el}/T = \gamma_{res} + A \exp(-\Delta/T)$, where γ_{res} is the residual Sommerfeld coefficient from the non-superconducting fraction of the sample and the second term is a phenomenological exponential decay expected for a gapped (s -wave superconductor) system. The fit shown in Fig. 2 (b) as the solid curve through the data below $T = 0.5$ K, gave the value $\gamma_{res} = 0.4$ mJ/mol K². With the total $\gamma = 6.01$ mJ/mol K², this suggests that $\approx 7\%$ of the sample volume is non-superconducting. An excellent fit of the low temperature C_{el} data to an exponential dependence suggests a conventional s -wave superconducting order parameter.

The magnitude of the anomaly in heat capacity at the superconducting transition is another measure of the nature (weak or strong coupling, single or multi-gap) of superconductivity. From the data in Fig. 2 (b) we estimate $\Delta C/\gamma T_c \approx 1.52$, which is close to the value 1.43 expected for a conventional, weak-coupling, single gap BCS superconductor. This further supports the conventional nature of superconductivity in PdTe₂.

Heat capacity measurements at various magnetic fields are shown in Fig. 3. As expected, the superconducting transition temperature is monotonically suppressed to lower temperatures and its magnitude becomes smaller at higher fields. From an equal entropy construction for the $C(T)$ data at each H , we extract the T_c at that H

and use it to draw a critical-field H_c versus temperature ($H_c - T$) phase diagram. The $H_c - T$ phase diagram is shown in Fig. 4 and follows a conventional behaviour expected for a BCS superconductor. In particular, we

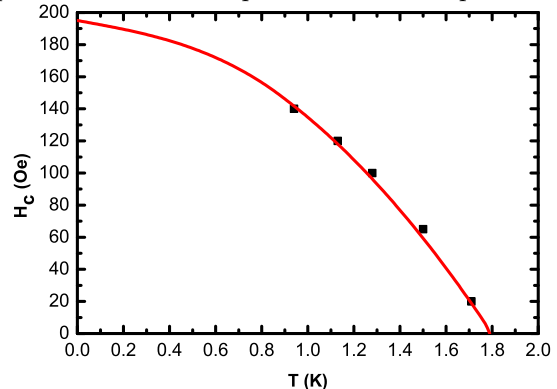


FIG. 4. (Color online) The critical magnetic field H_c versus temperature T phase diagram extracted from the C versus T data measured at various H shown in Fig. 3. The solid curve through the data is a fit by a phenomenological dependence (see text for details).

were able to fit the data with the phenomenological expression $H_c(T) = H_c(0)[1 - (T/T_c)^2]$, with the $T = 0$ critical field $H_c(0)$, and the critical temperature T_c as fit parameters. The fit shown as the solid curve through the data in Fig. 4 gave the values $H_c(0) = 195(2)$ Oe and $T_c = 1.78$ K, respectively.

Summary and Discussion: PdTe₂ is an interesting material where a superconducting state below $T_c \approx 1.7$ K coexists with a Topological band structure. Specifically, PdTe₂ has previously been shown to be a Type-II Dirac semi-metal raising the possibility of hosting a Topological superconducting state. In this study we have used thermodynamic measurements on high quality single crystals of PdTe₂ to probe the nature of the superconductivity. Our heat capacity measurements confirm bulk superconductivity at $T_c = 1.7$ K and show that the anomaly at T_c is characterized by the ratio $\Delta C/\gamma T_c \approx 1.5$ which is close to the value 1.43 expected for a weak-coupling, single-band BCS superconductor. The electronic contribution to the heat capacity C_{el} at the lowest temperatures shows an exponential T dependence which points to a gapped s -wave superconductivity. Additionally, the critical field versus temperature phase diagram shows a behaviour expected for a conventional superconductor. Therefore, all our results strongly indicate that inspite of the presence of a Topological band in the electronic band-structure of PdTe₂ which contributes to the transport properties, the superconductivity in PdTe₂ is completely conventional and has no Topological character.

Acknowledgments.— We thank the X-ray and SEM facilities at IISER Mohali.

-
- ¹ Masatoshi Sato and Yoichi Ando, Rep. Prog. Phys., **80**, 076501 (2017).
- ² J. Alicea, Rep. Prog. Phys. **75**, 076501 (2012).
- ³ S. R. Elliot, M. Franz, Rev. Mod. Phys. **87**, 137 (2015).
- ⁴ Y. S. Hor, A. J. Williams, J. G. Checkelsky, P. Roushan, J. Seo, Q. Xu, H. W. Zandbergen, A. Yazdani, N. P. Ong, and R. J. Cava, Phys. Rev. Lett. **104**, 057001 (2010).
- ⁵ M. Kriener, K. Segawa, Z. Ren, S. Sasaki, and Y. Ando, Phys. Rev. Lett. **106**, 127004 (2011).
- ⁶ Z. Liu, J. Am. Chem. Soc. **137**, 10512 (2015).
- ⁷ T. Asaba, Phys. Rev. X **7**, 011009 (2017).
- ⁸ Y.S. Hor, J.G. Checkelsky, D. Qu, N. P. Ong, R. J. Cava, Phys. J. Chem. Solids **72**, 572 (2011).
- ⁹ Amit and Yogesh Singh, J. Supercond. Novel Mag. **29**, 1975 (2016).
- ¹⁰ A. S. Erickson, J. -H. Chu, M. F. Toney, T. H. Geballe, and I. R. Fisher, Phys. Rev. B **79**, 024520 (2009)
- ¹¹ G. Balakrishnan, L. Bawden, S. Cavendish, and M. R. Lees, Phys. Rev. B **87**, 140507 (2013).
- ¹² J. L. Zhang, S. J. Zhang, H. M. Weng, W. Zhang, L. X. Yang, Q. Q. Liu, S. M. Feng, X. C. Wang, R. C. Yu, L. Z. Cao, L. Wang, W. G. Yang, H. Z. Liu, W. Y. Zhao, S. C. Zhang, X. Dai, Z. Fang, and C. Q. Jin, PNAS **108**, 24 (2011).
- ¹³ G. M. Luke, et al. Nature **394**, 558 (1998).
- ¹⁴ Sau et al. Phys. Rev. Lett. **104**, 040502 (2010).
- ¹⁵ J. Alicea Phys. Rev. B **81**, 125318 (2010).
- ¹⁶ V. S. Pribiag, A.J. A. Beukman, F. Qu, M. C. Cassidy, C. Charpentier, W. Wegscheider, and L. P. Kouwenhoven, Nature Nanotechnology **10**, 593 (2015).
- ¹⁷ C. Beenakker, and L. Kouwenhoven, Nature Physics **12**, 618 (2016).
- ¹⁸ L. Aggarwal, et al. Nature Materials **15**, 32 (2016).
- ¹⁹ H. Wang, H. Wang, H. Liu, H. Lu, W. Yang, S. Jia, X. J. Liu, X. C. Xie, J. Wei and J. Wang, Nature Materials **15**, 38 (2016).
- ²⁰ S. Das, L. Aggarwal, S. Roychowdhury, M. Aslam, S. Gayen, K. Biswas, and G. Sheet, Appl. Phys. Lett. **109**, 132601 (2016).
- ²¹ H. Huang, S. Zhou, and W. Duan, Phys. Rev. B **94**, 121117 (2016).
- ²² H. J. Noh, J. Jeong, and E. J. Cho, Phys. Rev. Lett. **119**, 016401 (2017).
- ²³ F. Fei, et al. Phys. Rev. B. **96**, 041201 (2017).
- ²⁴ M. Yan, et al., Nat. Commun. **8**, 257 (2017).
- ²⁵ A. A. Soluyanov, D. Gresch, Z. Wang, Q. Wu, M. Troyer, X. Dai, and B. A. Bernevig, Nature **527**, 495 (2015).
- ²⁶ H. Weng, C. Fang, Z. Fang, B. A. Bernevig, and X. Dai, Phys. Rev. X **5**, 011029 (2015).
- ²⁷ S.-Y. Xu et al., Science **349**, 6248 (2015).
- ²⁸ K. Deng, et al., Nature Phys. **12**, 1105 (2016).
- ²⁹ L. Huang, et al., Nat. Mater. **15**, 1155 (2016).
- ³⁰ J. Jiang, et al., Nat. Commun. **8**, 13973 (2017).
- ³¹ F. Jellinek, Arkiv. Kemi **20**, 447 (1963).
- ³² S. Das, et al., arXiv:1712.03749v1 (2017).
- ³³ T. R. Finlayson, Phys. Rev. B. **33**, 2473 (1986).